Volume 11 | Number 4 | 21 February 2024

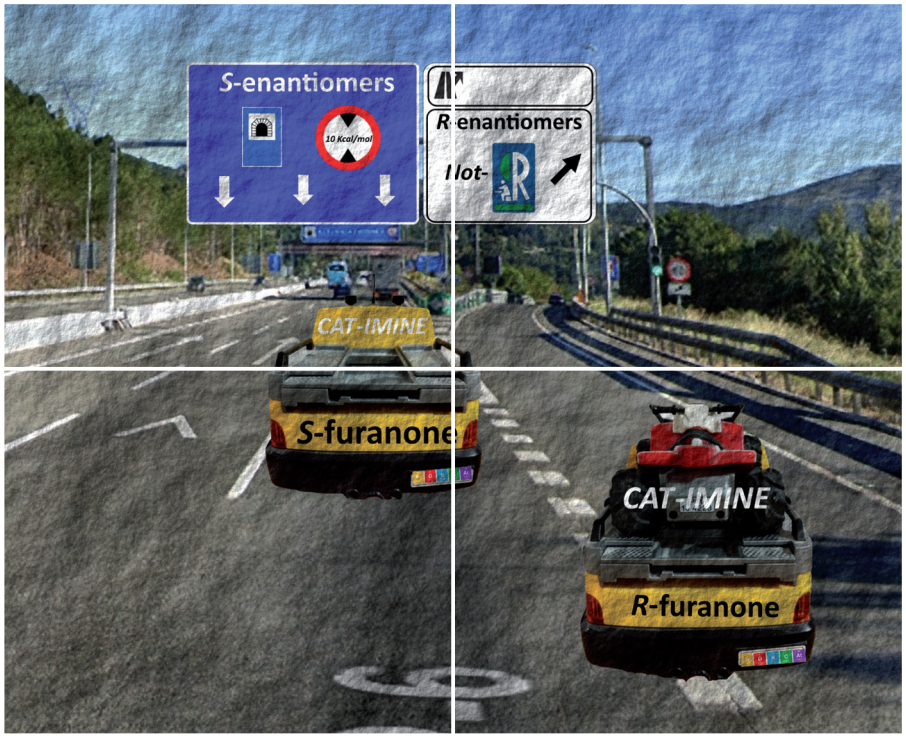

ORGANIC CHEMISTRY

FRONTIERS

CCS 中国化学会 CHINESE CHEMICAL SOCIETY
SIOC 1950
ROYAL SOCIETY OF CHEMISTRY
rsc.li/frontiers-organic

ORGANIC CHEMISTRY FRONTIERS

RESEARCH ARTICLE

View Article Online
View Journal | View Issue

Cite this: *Org. Chem. Front.*, 2024, **11**, 1028

Intramolecular hydrogen bond activation for kinetic resolution of furanone derivatives by an organocatalyzed [3 + 2] asymmetric cycloaddition†‡

Miguel A. Valle-Amores, [a] Claudia Feberero,[a,b] Ana Martin-Somer, [c] Sergio Díaz-Tendero, [d,e,f] Andrew D. Smith, [g] Alberto Fraile *[a,e] and José Alemán *[a,e]

Received 11th September 2023,
Accepted 10th October 2023

DOI: 10.1039/d3qo01471a

rsc.li/frontiers-organic

Herein, a formal highly enantioselective organocatalyzed [3 + 2] cycloaddition of furanone derivatives and azomethine ylides is presented. The success of this reaction resides in intramolecular hydrogen bond activation through an *o*-hydroxy group at the aromatic ring of the imine, allowing the formation of highly multifunctional bicyclic adducts with five stereogenic centers in a stereocontrolled manner. Furthermore, the reaction is paired with a highly efficient kinetic resolution of butenolides, achieving selectivity factors above 200. Using this methodology, furan-2(5*H*)-ones and furo[3,4-*c*]pyrrolidinones were obtained with high enantioselectivities. Quantum chemistry calculations reveal the crucial role of the hydrogen bond formed between the catalyst donor-units and the two reactants, which modifies their arrangement and promotes effective facial discrimination resulting in a highly selective kinetic resolution. In addition, further applicability of the kinetic resolution process is shown.

Introduction

The synthesis of chiral compounds in an efficient way has been and still is one of the principal issues within the organic community in both industrial and academic points of view. Among the numerous methods that exist at present, kinetic resolution (KR) is one of the most powerful tools used since it allows, in a very efficient way, the separation of both enantiomers from racemic mixtures.[1]

Regarding the different processes of kinetic resolution, we can distinguish between the use of chiral auxiliaries[1c,2] and catalysts.[1c,3] The principle of KR relies on the reaction of a chiral reagent or catalyst with each enantiomer of the racemic mixture that proceeds through the generation of two diastereomeric transition states. The difference in the free energy between these transition states ($\Delta\Delta G^{\ddagger}$) dictates the difference in rate constants (k) for the reaction of each enantiomer, allowing their discrimination and determination of the efficiency of the KR using the selectivity factor (s) values.[4] The catalytic KR can be divided into enzymatic,[5] which has long been a popular strategy, and non-enzymatic processes,[6] which include both metal catalysis[7] and organocatalysis.[8]

Within the plethora of reactions studied for the catalytic kinetic resolution of racemates, [3 + 2] cycloadditions have been scarcely studied. The first example was described by Fu's group in 2005, who carried out the kinetic resolution of azomethine imines with activated alkynes catalysed by a chiral copper complex, achieving high enantioselectivities of the recovered dipole and with selectivity factors from 15 to 96 (Scheme 1a).[9] Subsequently, other authors have published metal-catalyzed [3 + 2] kinetic resolution processes of different racemic dipolarophiles, reaching high ee and s values.[10] Regarding organocatalyzed [3 + 2] cycloadditions, to date,

[a]*Organic Chemistry Department (Módulo 1), Facultad de Ciencias, Universidad Autónoma de Madrid, 28049 Madrid, Spain. E-mail: alberto.fraile@uam.es, jose.aleman@uam.es; https://www.uam.es/jose.aleman*
[b]*Organic Chemistry Area, Chemistry Department, Universidad de Burgos, Burgos 09001, Spain*
[c]*Applied Physical Chemistry Department (Módulo 14), Facultad de Ciencias, Universidad Autónoma de Madrid, 28049 Madrid, Spain*
[d]*Chemistry Department (Módulo 13), Facultad de Ciencias, Universidad Autónoma de Madrid, 28049 Madrid, Spain*
[e]*Institute for Advanced Research in Chemical Sciences (IAdChem), Universidad Autónoma de Madrid, 28049 Madrid, Spain*
[f]*Condensed Matter Physics Center (IFIMAC), Universidad Autónoma de Madrid, 28049 Madrid, Spain*
[g]*EaStCHEM, School of Chemistry, University of St Andrews, North Haugh, Fife, Scotland, KY16 9ST, UK*

†Dedicated to M. Rosario Martín Ramos for her great contributions to the 5-alkoxyfuran-2(5*H*)-one chemistry.

‡Electronic supplementary information (ESI) available. CCDC 2160961. For ESI and crystallographic data in CIF or other electronic format see DOI: https://doi.org/10.1039/d3qo01471a

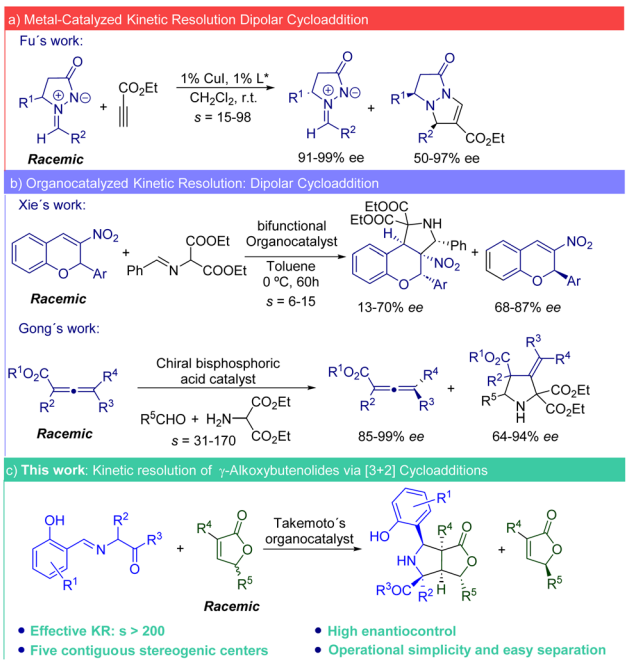

Scheme 1 Catalyzed kinetic resolution by dipolar cycloaddition reactions.

there are only two precedents. The first was reported by Xie's group in 2010, who carried out the [3 + 2] cycloaddition of azomethine ylides to nitroolefins catalyzed by Takemoto's organocatalyst. While this procedure provided the KR of racemic 2-nitro-2*H*-chromene derivatives, the enantioselectivities obtained were from low to moderate (top, Scheme 1b).[11] The second example relates to the three-component kinetic resolution catalysed by chiral bisphosphoric acids between racemic 2,3-allenoates and *in situ* formed azomethine ylides. In this case, 3-methylenepyrrolidine derivatives were obtained with high enantioselectivities (up to 94% ee) with the (*R*)-2,3-allenoates recovered in excellent enantioselectivities (up to 99% ee) (bottom, Scheme 1b).[12] It should be noted that in both precedents, the authors must make use of azomethine ylide precursors that bear two electron-withdrawing (two esters are present) groups in the methylene carbon of imine which, inevitably, limits the structure of the final products.

On the other hand, furanones, a five-membered ring containing an oxygen atom, are a class of heterocyclic compounds of widespread interest in the organic, pharmacological and biological fields, containing diverse biological properties such as analgesic, anti-inflammatory, and anticancer properties among others.[13]

Some of the most used synthons that present the butenolide structure are the 5-alkoxyfuran-2(5*H*)-ones which allow achieving new approaches to acyclic and heterocyclic products.[14,15] Feringa[14c,16] and others[15,17,18] have used butenolide derivatives with chiral auxiliaries such as menthol or sulfinyl groups to achieve diastereoselective asymmetric processes. Starting from these chiral precursors, many interesting structures with high diastereoselectivities have been synthesized. While demonstrative, green chemistry principles consider the use of chiral auxiliaries as not efficient or atom economical, emphasizing the need to develop effective catalytic processes.[19] Therefore, the development of new catalytic procedures to carry out asymmetric reactions with 5-alkoxyfuran-2(5*H*)-ones would be highly desirable. Taking into account the scarce number of examples of organocatalyzed [3 + 2] kinetic resolution and the high synthetic value of furan-2(5*H*)-ones, we hypothesized that an efficient kinetic resolution could be achieved by following a match/mismatch[20] process using a bifunctional organocatalyst and intramolecular hydrogen bond activation (Scheme 1c).[21]

Results and discussion

Initially, to determine the influence of the hydroxyl group at the imine, we carried out the cycloaddition of the 5-methoxy-2(5*H*)-furanone **(±)-2a** with imines **1a** (R = H) and **1b** (R = OH) in the presence of 20 mol% of Takemoto's catalyst **3a**, obtaining better conversion and enantioselectivity with imine **1b** (Scheme 2). In addition, the reaction with imine **1a** led to a mixture of diastereoisomers (3 : 1) while with **1b** only one diastereoisomer **4b** was achieved. These results bring to light the important role of the hydroxyl group at the imine in the reactivity and stereoselectivity of this asymmetric process.[21b,c,22] Furthermore, it is remarkable that the selectivity factor (*s*) and the conversion (*c*) are very high, highlighting the effectiveness of the kinetic resolution of **(±)-2a** (see Table 1, entry 1).

Having determined that using imine **1b** affords high selectivity, we continued looking for the optimal reaction conditions. Thus, different bifunctional organocatalysts (20 mol%) were studied, with Takemoto's thiourea catalyst **3a** giving the highest selectivity for this cycloaddition reaction (compare entry 1 with entries 3–8, Table 1). Notably, a racemic background reaction was not operative, as no conversion to the product was obtained in the absence of catalyst **3a** (entry 2). The use of squaramide-based catalysts led to a dramatic loss in conversion (entries 4 and 8). Interestingly, the *pseudo*-enantiomer catalyst **3e** gave very low conversion in comparison with the organocatalyst **3b**. Having identified the most promising catalyst, different solvents were screened (entries 9–12). The use of dichloromethane and *tert*-butylmethylether (entries 9 and 11, respectively) afforded reduced product conversions

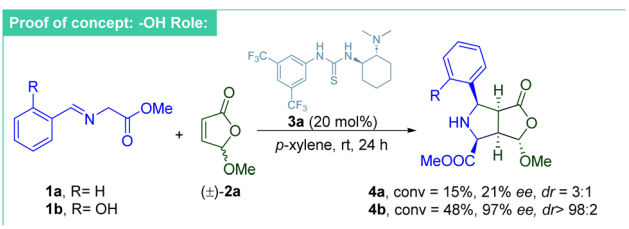

Scheme 2 Proof of concept for the intramolecular H-bond activation: OH role. The reactions were run with 0.1 mmol of imine **1** and 0.1 mmol of **(±)-2a** in 0.3 mL of *p*-xylene ([0.33] M).

Table 1 Screening of reaction conditions[a]

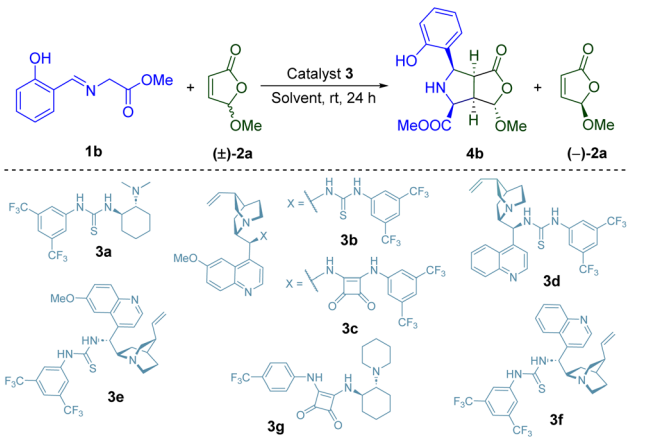

Entry	Cat (mol%)	Solvent	Conv.[b] (%)	ee **4b**[c] (%)	ee **(−)-2a**[c] (%)	s[d] (c (%))
1	**3a (20)**	***p*-Xylene**	**48**	**97**	**87**	**190 (47)**
2	—	*p*-Xylene	<5	—	—	—
3	**3b** (20)	*p*-Xylene	40	96	65	100 (40)
4	**3c** (20)	*p*-Xylene	10	—	—	—
5	**3d** (20)	*p*-Xylene	20	—	—	—
6	**3e** (20)	*p*-Xylene	18	—	—	—
7	**3f** (20)	*p*-Xylene	19	—	—	—
8	**3g** (20)	*p*-Xylene	<5	—	—	—
9	**3a** (20)	CH_2Cl_2	34	86	50	22 (37)
10	**3a** (20)	Et_2O	47	95	91	120 (49)
11	**3a** (20)	MTBE	45	91	82	50 (47)
12	**3a** (20)	Toluene	48	92	98	110 (51)
13[e]	**3a** (20)	*p*-Xylene	45	95	81	100 (46)
14	**3a** (15)	*p*-Xylene	42	97	76	150 (44)
15	**3a** (10)	*p*-Xylene	38	97	55	110 (36)
16[f]	**3a** (20)	*p*-Xylene	48	97	92	>200 (49)
17[g]	**3a** (20)	*p*-Xylene	40	95	68	80 (41)

[a] The reaction was run with 0.1 mmol of imine **1b** and 0.1 mmol of **(±)-2a** in 0.3 mL of indicated solvent ([0.33] M). [b] Conversion determined by ^{1}H NMR. [c] Determined by chiral SFC. [d] Calculated conversion (c) = $ee_{SM}/(ee_{SM} + ee_{PR})$, selectivity factor ($s$) = $\ln[(1 - c)(1 - ee_{SM})]/\ln[(1 - c)(1 + ee_{SM})]$. [e] [0.16] M instead of [0.33] M. [f] The reaction was scaled up to 1.0 mmol of imine **1b**. [g] The reaction was carried out with 0.05 mmol of imine **1b**.

and enantioselectivities, and hence lower selectivity factors (s) than with *p*-xylene (entry 1). However, the reaction in diethylether and toluene (entries 10 and 12) gave rise to good conversion and enantioselectivity, but reduced s. Considering the data obtained, *p*-xylene was selected as the best solvent to continue the reaction screening. Subsequently, reaction concentration was also tested, with the highest selectivity at [0.33] M (entry 1) instead of [0.16] M (entry 13) (see the ESI‡). Finally, the catalyst loading was studied, with reduced product conversions and selectivity factors (s) observed when using 15 and 10 mol% catalyst (entries 14 and 15). The reaction was also scaled up to 1.0 mmol, with no detrimental effect on the stereoselectivity and obtaining the best results in terms of both enantiomeric excess and selectivity factor (**4b**: 47% and **2a**: 46% yield, entry 16). Additionally, to determine if the use of a lower amount of imine **1b** could provide similar results to that shown in entry 1, we carried out the reaction starting from 0.05 mmol of **1b** (entry 17). However, the results obtained were worse, achieving only a 68% enantiomeric excess for furanone **(−)-2a** and a lower selectivity factor for the kinetic resolution.

With the optimized conditions in hand (c = 47%, s = 190, Table 1, entry 1), the scope of the dipolar cycloaddition and the efficiency of the KR for **(±)-2a** were evaluated (Scheme 3). For this purpose, a large assortment of imines **1** bearing an *ortho*-hydroxyl group at the aromatic ring and with different substituents were tested. When electron-donating groups are present at the aromatic ring of the imine such as the methyl (**1c** and **1d**) or methoxy (**1e** and **1f**) group, cycloaddition products **4c–f** were obtained with high conversions and excellent enantioselectivities (94–99% ee). Moreover, the (*R*)-5-methoxyfuran-2(5*H*)-one **(−)-2a** could be recovered with high yields and good enantioselectivities (86–90% ee), achieving excellent selectivity factor values (s > 200) for **1c–e**, while for **1f** a reduced but still significant value was obtained (s = 90). However, the presence of a diethylamino group (**1g**) maintained the enantioselectivity of the cycloaddition (98% ee, s = 170) but led to decreased conversion (c = 25%). Furthermore, halogens at *para*- (**1h–i**) and *meta*-positions (**1j**) were employed. Cycloaddition products **4h–j** were obtained with good conversions and high enantioselectivities (up to 95% ee for **4i**). Regrettably, enantioselectivities of the recovered starting material **(−)-2a** were from moderate to good (up to 87% ee), affording reasonable selectivity factors (s = 28–80) for the resolution of **(±)-2a**. When a nitro group is present at the *meta* position (**1k**), the cycloadduct **4k** and the furanone **(−)-2a** were obtained with excellent enantiomeric excess (95 and 90% ee, respectively) and, more importantly, the conversion (c = 49%) and the selectivity factor (s = 120) were very high. An ester group at the *meta* position (**1l**) afforded the cycloaddition product **4l** with good enantioselectivity (91% ee), but with a decreased conversion and selectivity factor (c = 38%, s = 37). Two iminoesters with a naphthyl group (**1m** and **1n**) were reacted at room temperature with the dipolarophile **(±)-2a** under the standard reaction conditions without obtaining the corresponding cycloadducts. To our delight, this limitation could be overcome by increasing the temperature to 50 °C, achieving thus **4m** and **4n** with excellent enantioselectivity values (93 and 97% ee, respectively) and with a high selectivity factor for both reactions (s = 90). Notably, alpha-substituted imines **1o** and **1p**, with a methyl or a phenyl group, respectively, worked well and allowed the asymmetric synthesis of 4-substituted pyrrolidines **4o** and **4p**, bearing a quaternary stereocentre, with good enantioselectivities (87 and 71% ee, respectively), high or complete diastereoselectivity (for **4p**: 5 : 1 dr) and increased conversion (up to 51%). Nevertheless, regarding the selectivity, the resolution was more effective with the α-methyl imine **1o** (s = 45) than with the α-phenyl ring **1p** (s = 11). Different electron-withdrawing groups at the imine moiety, such as *N*,*N*-dimethyl amide **1q**, ethyl ester **1r**, and Weinreb's amide **1s**, also led to the corresponding bicyclic adducts **4q–s** in good to high enantioselectivities (84–93% ee) and high conversions. The best results in terms of selectivity

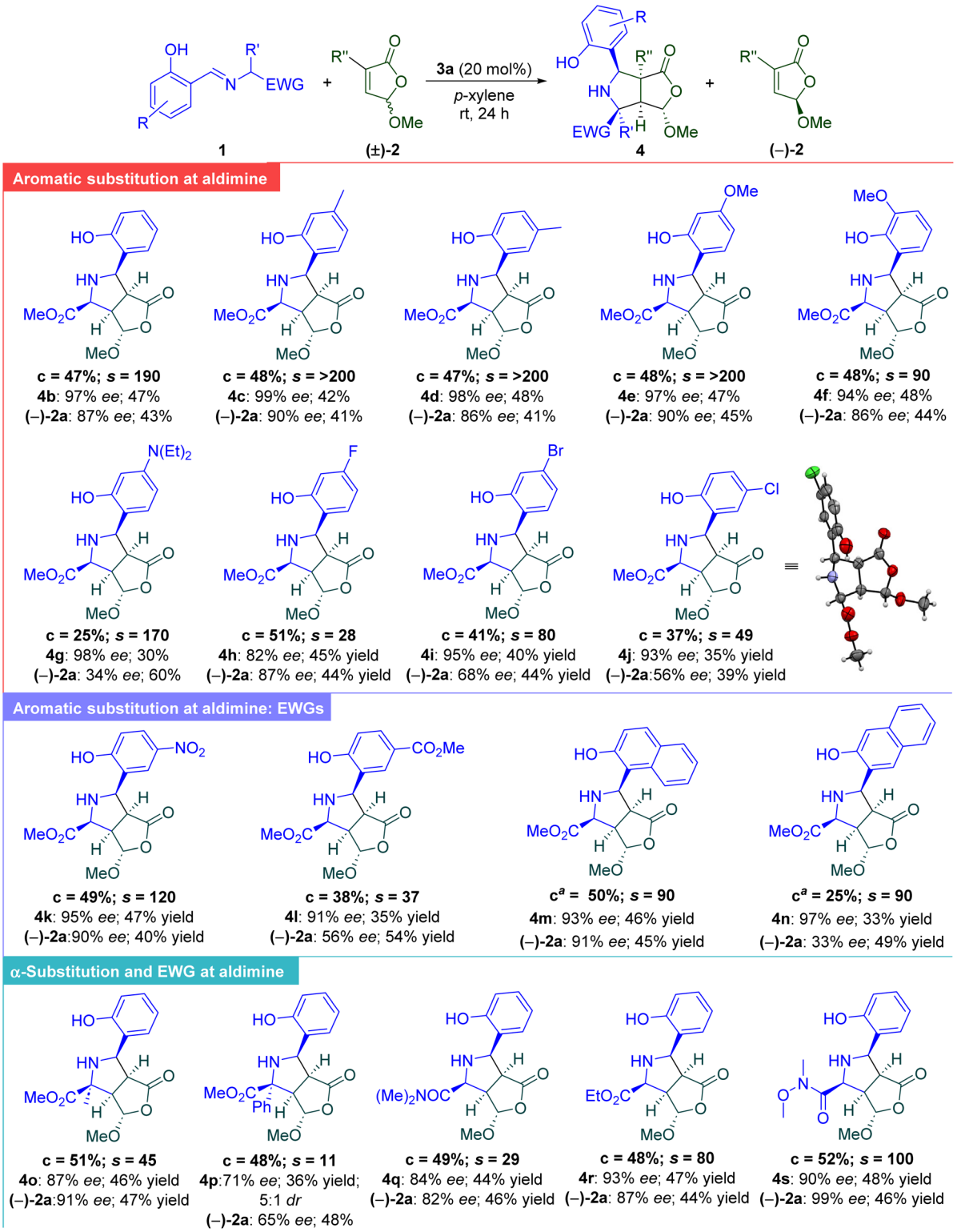

Scheme 3 Scope of the [3 + 2] cycloaddition kinetic resolution. Reaction conditions: **1** (0.1 mmol), (±)-**2** (0.1 mmol), **3a** (20 mol%), *p*-xylene (0.3 mL), rt for 24 h unless otherwise noted. Isolated yields are shown. Enantiomeric ratio was measured by SFC. Calculated conversion (*c*) = $ee_{SM}/(ee_{SM} + ee_{PR})$. Selectivity factor (*s*) = $\ln[(1 - c)(1 - ee_{SM})]/\ln[(1 - c)(1 + ee_{SM})]$. [a]Reaction was carried out at 50 °C for 2 days.

factor were achieved from Weinreb's amide **1s** (*s* = 100), which allowed recovery of the (*R*)-5-methoxyfuran-2(5*H*)-one **(–)-2a** with excellent enantioselectivity (99% ee). The absolute configuration of the stereogenic centres of the hydroxylated cycloadducts **4** was assigned by X-ray crystallographic analysis of a monocrystal of **4j** (3*S*,3a*R*,4*S*,6*R*,6a*S*)[23] (middle, Scheme 3) and

assuming the same stereochemical outcome for the rest of the products.

Finally, to demonstrate the versatility of our [3 + 2] cycloaddition kinetic resolution, we studied the influence of the incorporation of a variety of substituents at C(3) and C(5) within the furan-2(5*H*)-one as well as the use of 2-(5*H*)-pyrrolones (Scheme 4). Varying the substituent at C(5) from the methoxy to ethoxy group gave excellent conversion to the product, giving an *s* factor >200 for the kinetic resolution, and provided resolved (*R*)-5-ethoxyfuran-2(5*H*)-one **(−)-2b** in excellent enantiomeric excess.

Introducing a thiolate group resulted in the successful formation of the cycloadduct **4u** with a high degree of enantioselectivity (92% ee). However, the furanone **2c** was obtained with no enantioselectivity. This observation can be attributed to the high acidity of the thioacetal proton (H-5) in furanone **2c**, which can lead to complete epimerization in the presence of organocatalyst **3a**, resulting in a racemic mixture, followed by auto-selfcondensation as it was previously described in the literature.[24] The reaction with a more reactive *pseudo* ester such as the 3-bromo-5-methoxyfuran-2(5*H*)-one **(±)-2d** was studied under the optimized conditions, achieving the cycloadduct **4v** with good enantioselectivity (87% ee) and moderate conversion (*c* = 35%) and selectivity. The reactions with the aromatic derivative **(±)-2e** worked well, giving rise to the cycloadduct **4w** with good selectivity, while the heteroaromatic species **(±)-2f** gave the cycloadduct **4x** in excellent enantioselectivity (*s* = 120), but with low conversion, accounting for the recovery of the pyrrole derivative **(−)-2f** in low enantiomeric excess. With the incorporation of an alkenyl group the cycloaddition reaction was facile, leading to the formation of the corresponding adduct **4y** and the pseudoester **(−)-2g** with excellent enantioselectivities and yields. Notably, in these recent examples, it was possible to generate a quaternary carbon stereocenter in a precisely controlled manner. In contrast, we also studied the reactivity of 5-methoxypyrrol-2(5*H*)-ones containing an acetyl substituent at the nitrogen atom. Regrettably, under the specified conditions the acetyl derivative (±)-**2h** reacted to give the lactam **4z** and 2-(5*H*)-pyrrolone **2h** in high yield, but as a racemic mixture. Furthermore, attempts were made to conduct [3 + 2] cycloaddition reactions using 5-methoxyfuran-2(5*H*)-ones containing a methyl substituent at the alpha position. However, no conversion was observed in these reactions.

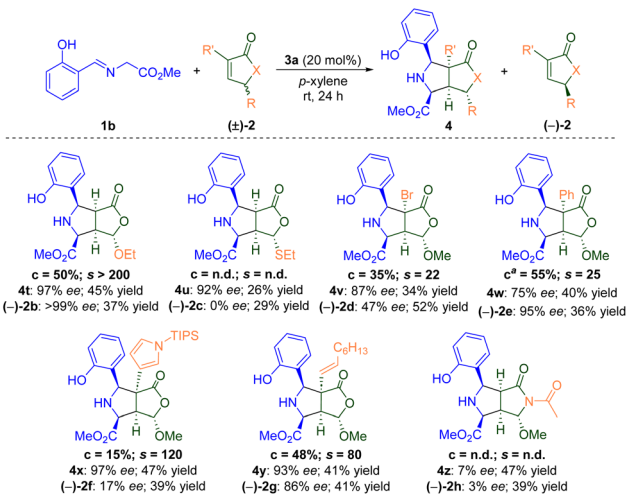

Scheme 4 Scope of the [3 + 2] cycloaddition kinetic resolution regarding furanone and its derivatives. Reaction conditions: **1** (0.1 mmol), **(±)-2** (0.1 mmol), **3a** (20 mol%), *p*-xylene (0.3 mL), rt for 24 h unless otherwise noted. Isolated yields are shown. Enantiomeric ratio was measured by SFC. Calculated conversion (*c*) = $ee_{SM}/(ee_{SM} + ee_{PR})$. Selectivity factor (*s*) = $\ln[(1 - c)(1 - ee_{SM})]/\ln[(1 - c)(1 + ee_{SM})]$. [a]Reaction was carried out at 0 °C in toluene.

Considering the excellent results obtained in the kinetic resolution of 5-methoxyfuran-2(5*H*)-one **(±)-2a** and to showcase the utility of the developed process, we envisioned the use of the enantioenriched isomer **(−)-2a** as the starting material for new asymmetric reactions (Scheme 5). Thus, the crude reaction product obtained during the [3 + 2] cycloaddition was submitted to a *one-pot* procedure. Therefore, several Michael additions[14g] and a [3 + 2] cycloaddition[18b] were carried out to demonstrate the applicability of our methodology (Proc. A, Scheme 5). Thus, the addition of (*R*)-1-phenylethan-1-amine or thiophenol to the crude reaction mixture from the cycloaddition (equations a and b) afforded the corresponding aza-Michael or *thio*-Michael products (**5** and **6**, respectively) with excellent *enantio*- and diastereo-selectivity and in high yields (only 50% of the final product can be obtained). Furthermore, the addition of 11*H*-dibenzo[*b*,*e*]azepine 5-oxide led to the cycloadduct **7** with excellent results (equation c).

Finally, to corroborate the configurational stability of furanone, the same reactions showed before, starting from the cycloaddition reaction crude products, were conducted from the (*R*)-5-methoxyfuran-2(5*H*)-one **(−)-2a** obtained by kinetic resolution and the subsequent purification by flash chromatography on silica gel (Proc. B, Scheme 5). The enantiomeric excesses achieved in these transformations brought to light that the 5-methoxyfuran-2(5*H*)-one **(−)-2a** obtained by kinetic resolution is configurationally stable and can be isolated in the enantioenriched form without any racemization.

Mechanistic proposal

Once the scope of this organocatalyzed [3 + 2] asymmetric cycloaddition and the synthetic applicability of this kinetic resolution were demonstrated, we wished to rationalise the stereochemical outcome of this process. Taking into account the absolute configuration of final adducts **4**, an *endo* approach of ylide **1** in its *anti*-conformation to the less hindered face of the furanone **2** (*anti-approach*) takes place. To corroborate this proposal, quantum chemistry calculations were carried out to obtain further theoretical insights into the enantioselectivity of the reaction.[25] We initially considered the possible relative orientations between catalyst **3a** and reactants **1b** and **(±)-2a**. Thus, we followed a similar strategy to that previously proposed,[26] which consists of a systematic exploration

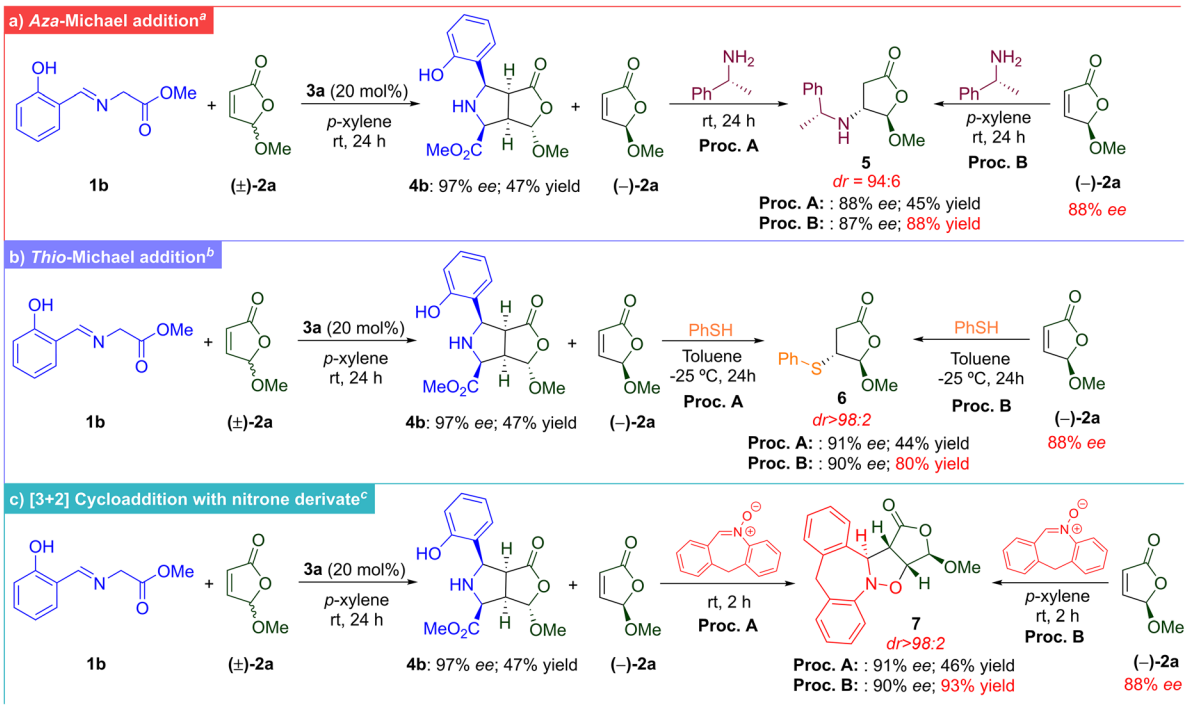

Scheme 5 Further derivatization of **(–)-2a** in one pot and direct procedures. One-pot (**Proc. A**) and direct (**Proc. B**) procedures: [a]aza-Michael addition of (*S*)-1-phenylethanamine to resolved **(–)-2a**. [b]thio-Michael addition of thiophenol to resolved **(–)-2a**. [c][3 + 2] cycloaddition of nitrone to resolved **(–)-2a**. Reactions were carried out at the 0.1 mmol and 0.05 mmol scale for procedure A and B, respectively.

of the potential energy surface (PES) using the GFN2-xTB method[27] as implemented in the CREST code.[28] From the most stable structures found with this method, the PES was refined using density functional theory (DFT) calculations, by combining the B3LYP functional and the 6-31+G(d,p) basis set, and including dispersion forces through the D3 version of Grimme's method with the Becke–Johnson damping.[29] These calculations were carried out with the Gaussian 16 code.[30]

The reaction was studied considering the *endo* approach for the two enantiomers of **2** (*exo* approaches were discarded since they are less favourable than the *endo* ones,[15c,21b] see the ESI‡).[25] We considered a two-step process. The first step is the activation of the imine **1b** by an H transfer from **1b** to catalyst **3a**. In the second step, new C–C bonds are formed, yielding the 5-membered ring (Fig. 1 and 2, respectively). For both enantiomers, the H transfer requires ~18 kcal mol^{-1} from the initial pre-association complex, PAC (pre-H transfer: complex formed by the catalyst and the two reactants **1b** and **(±)-2a**) (Fig. 1). However, the main difference was found in the second cycloaddition step (Fig. 2). While for the TS leading to the formed cycloadduct a low barrier of ~3.5 kcal mol^{-1} is observed (black line), in the alternative case a transition state was located at a much higher energy, ~9 kcal mol^{-1} (blue line), than the initial pre-association-complex (PAC, Fig. 2); *i.e.*, even higher than the first TS for H transfer. Therefore, for the non-observed isomer, the much higher barrier for the cycloaddition prevents its formation, thus explaining the experimentally obtained adduct.

To obtain further molecular insights into the origin of the stereocontrol, we analysed the non-covalent interaction (NCI) at the second TS (TS CC, Fig. 3) by means of NCI plots, using the NCI code.[31] NCI plots show the different interaction regions using a colour code to rank those interactions. Red is used for destabilizing interactions, blue for stabilizing interactions and green for delocalized weak interactions. The intensity of these colours is associated with the interaction strength.

For both TSs, NCI plots revealed weak delocalized interactions (green) between the three moieties interacting (Fig. 3). However, the orientations of **1b** and both enantiomeric dipolarophiles **2a** with respect to the catalyst are slightly different, leading to different non-covalent interactions in the C–C bond forming transition state. TS-A (observed reaction) presents a strong NH···O hydrogen bond (blue flat circular region) between the ammonium group, generated after the H transfer to the catalyst, and the hydroxy group of ylide **1b** (top image in Fig. 3A). This leads to a stronger intramolecular hydrogen bond in **1b** between the hydroxy group and the iminic nitrogen (actually it appears as H bonded to both atoms). While for TS-B, this hydrogen bond is formed with the iminic nitrogen of **1b** (instead of the hydroxy group) and is weaker (only slightly blue) (top image in Fig. 3B). The significance of the hydroxyl group on the aromatic ring of the imine becomes apparent from these findings. It plays a crucial role in establishing a beneficial intermolecular interaction with the organocatalyst through hydrogen bonding. In contrast, the absence of this hydroxyl group in imine **1a** prevents such an

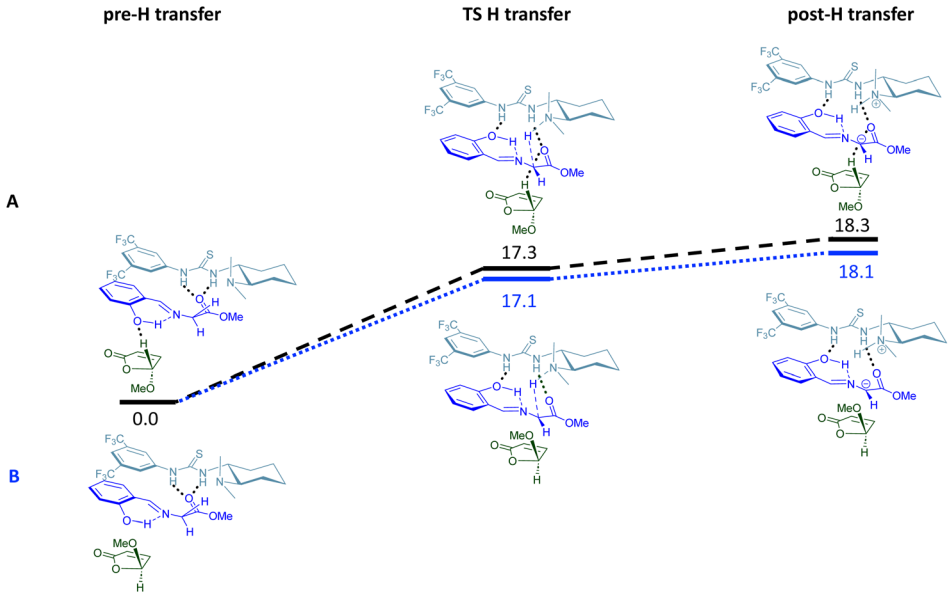

Fig. 1 Potential energy surface for the H transfer reaction and the structures corresponding to the stationary states, both for the path leading to the observed product (A) and the path for the not observed enantiomer (B). Relative Gibbs free energies in kcal mol^{-1} are referred to the pre-H transfer complex.

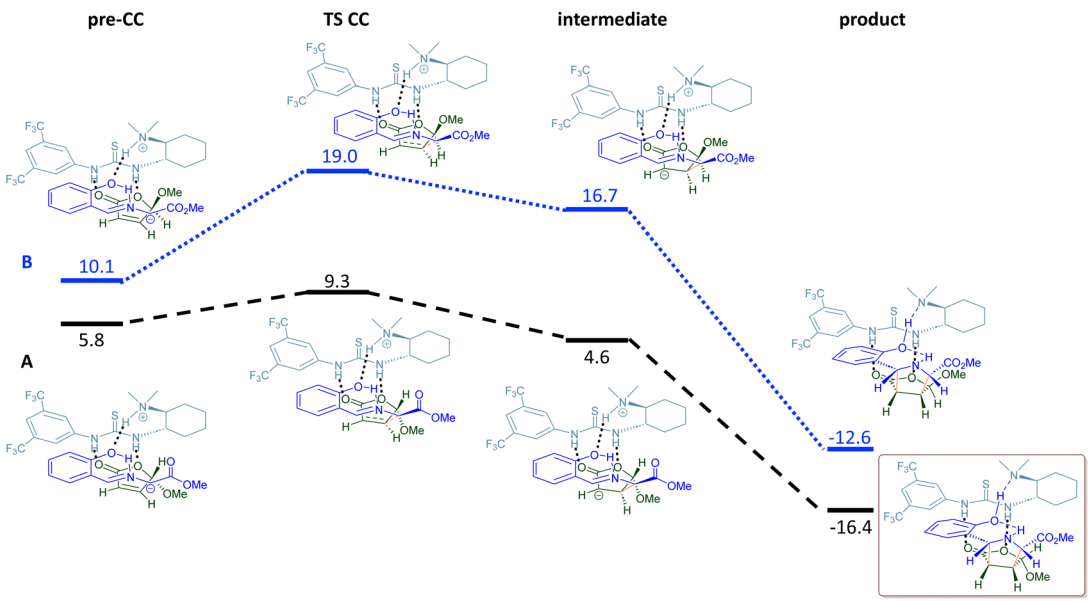

Fig. 2 Potential energy surface for the CC bond formation and the structures corresponding to the stationary states, both for the path leading to the observed product (A, black line) and the path for the not observed enantiomer (B, blue line). Relative Gibbs free energies in kcal mol^{-1} are referred to the pre-H transfer complex.

interaction, making it impossible to form a structured and organized complex between **1a** and **3a**. Consequently, this leads to low enantioselectivity.

Concerning the NCI between the catalyst and dipolarophile **2a**, at TS-A there are two hydrogen bonds between the thiourea group in the catalyst and oxygen atoms 1 and 2 in **(+)-2a**, with 1 being the stronger one (bottom image in Fig. 3A). For TS-B (not-formed adduct), the different orientation of the methoxy group of **(−)-2a** allows the formation of a very weak hydrogen bond (green) between carbonyl oxygen atom 1 in the ylide **1b** (bottom image in Fig. 3B) and the catalyst, displacing the furanone unit to the right.

This displacement leads to the formation of only one hydrogen bond between oxygen 2 in furanone **(−)-2a** (NH···O) and the catalyst, which is weaker than in TS-A (lighter blue color). In addition, for TS-B, there is a third CH···O bond (3), not

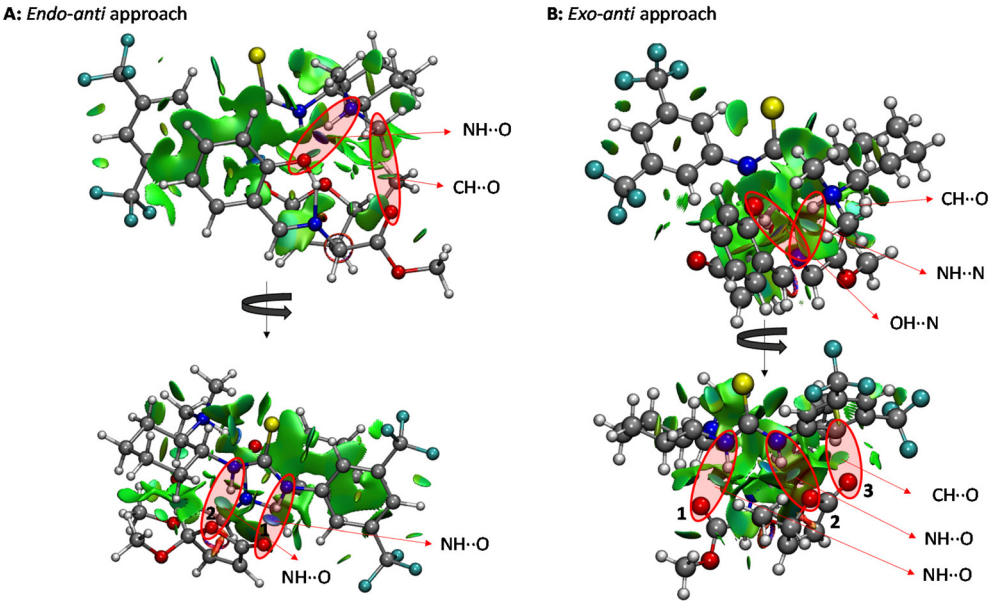

Fig. 3 Noncovalent interaction (NCI) plot for the C–C bond formation transition states leading to the observed product (A) and the isomer (B). The green, blue, and red regions, respectively, represent attractive, strongly attractive, and repulsive interactions.

present in TS-A, but it is very weak (green). The arrangement of the reactants at TS-B makes the region between the three moieties more crowded than in TS-A, hampering the approach of the two reactants to form the new C–C bond. This is reflected in a higher barrier for CC bond formation (TS-B energy is ~10 kcal mol^{-1} higher than that of TS-A).

Conclusions

In conclusion, in this work we report an organocatalyzed [3 + 2] enantioselective cycloaddition of formal azomethine ylides with racemic furan-2(5*H*)-ones. This allows the generation of highly functionalized and versatile bicyclic adducts with up to 5 contiguous stereogenic centres in a stereocontrolled *endo* approach and with high enantioselectivities (up to 99% ee) due to the presence of the hydroxyl group at the aromatic ring of imines. Moreover, this cycloaddition reaction is paired with an efficient kinetic resolution of the furan-2(5*H*)-one, leading to the resolved substrate in an enantioenriched form (up to 99% ee). This kinetic resolution takes place with selectivity factors up to 200 and very high conversions. DFT calculations have demonstrated the great effectiveness of the organocatalyzed [3 + 2] asymmetric cycloaddition to reach a very efficient kinetic resolution and the crucial influence of the hydroxyl group at the imine aromatic ring on the deprotonation process to generate the reactive ylide and on the stereoselectivity.

Data availability

Experimental details, general procedures, optimization of reaction conditions, characterization of products, copies of NMR and HPLC spectra of all products and computational details are provided in the ESI.‡

Author contributions

A. F. and J. A. conceived, designed, and supervised this work. M. A. V.-A. and C. F. performed the experiments and the synthesis and characterization of new compounds. A. M.-S. and S. D.-T. performed the calculations and wrote the theoretical part of the article. A. F. and M. A. V.-A prepared the ESI.‡ A. F., J. A., M. A. V.-A and A. D. S. wrote the article. All authors contributed to the discussion of the results.

Conflicts of interest

There are no conflicts to declare.

Acknowledgements

This work was supported by the Spanish Ministry of Science and Innovation (projects PID2019-110091GB-I00, PID2021-122299NB-I00, PID2022-138470NB-I00, TED2021-130470B-I00, and TED2021-129999B-C32), "Comunidad de Madrid" for European Structural Funds (S2018/NMT-4367), Proyectos Sinérgicos I + D (Y2020/NMT-6469), and "María de Maeztu" (CEX2018-000805-M) Program for Centers of Excellence in R&D. A. M. S. thanks the Madrid Government (Comunidad de Madrid – Spain) under the Multiannual Agreement with Universidad Autónoma de Madrid in the line Support to Young Researchers, in the context of the V PRICIT (SI3-

PJI-2021-00463). C. F. thanks Ministerio de Universidades for a Margarita Salas grant. In addition, the authors acknowledge the generous allocation of computer time at the Centro de Computación Científica at the Universidad Autónoma de Madrid (CCC-UAM).

References

1 (*a*) H. B. Kagan and J. C. Fiaud, in *Topic in Stereochemistry*, ed. E. L. Eliel and S. H. Wilen, John Wiley & Sons, Inc., 1988, ch. 4, vol. 18, pp. 249–330; (*b*) *Enantiomers, Racemates, and Resolutions*, ed. J. Jacques, A. Collet and S. H. Wilen, John Wiley & Sons, Inc., 1981; (*c*) *Separation of Enantiomers: Synthetic Methods*, ed. M. H. Todd, Wiley-VCH, Weinheim, Germany, 2014.

2 (*a*) X.-C. He and C.-Y. Qi, Practical Tactics in Resolution of Racemates via Diastereomeric Salt Formation, *Chin. J. Chem.*, 2007, **25**, 583–586; (*b*) M. R. Maddani, J.-C. Fiaud and H. B. Kagan, Stoichiometric Kinetic Resolution Reactions, in *Separation of Enantiomers: Synthetic Methods*, ed. M. H. Todd, Wiley-VCH, Weinheim, Germany, 2014, ch. 2, pp 13–74; (*c*) S.-Y. Hsieh, B. Wanner, P. Wheeler, A. M. Beauchemin, T. Rovis and J. W. Bode, Stereoelectronic Basis for the Kinetic Resolution of *N*-Heterocycles with Chiral Acylating Reagents, *Chem. – Eur. J.*, 2014, **20**, 7228–7231.

3 (*a*) H. Pellissier, Catalytic Kinetic Resolution, in *Separation of Enantiomers: Synthetic Methods*, ed. M. H. Todd, Wiley-VCH, Weinheim, Germany, 2014, ch. 3, pp. 75–122; (*b*) E. R. Jarvo and S. J. Miller, Acylation Reaction, in *Comprehensive Asymmetric Catalysis, Supplement 1*, ed. E. N. Jacobsen, A. Pfaltz and H. Yamamoto, Springer-Verlag Berlin, Heidelberg, 2004, ch. 43, pp. 189–206; (*c*) J. M. Keith, J. F. Larrow and E. N. Jacobsen, Practical Considerations in Kinetic Resolution Reactions, *Adv. Synth. Catal.*, 2001, **343**, 5–26.

4 M. D. Greenhalgh, J. E. Taylor and A. D. Smith, Best Practice Considerations for Using the Selectivity Factor, s, as a Metric for the Efficiency of Kinetic Resolutions, *Tetrahedron*, 2018, **74**, 5554–5560.

5 (*a*) A. Ghanem and H. Y. Aboul-Enein, Application of Lipases in Kinetic Resolution of Racemates, *Chirality*, 2005, **17**, 1–15; (*b*) M. T. Reetz, Biocatalysis in Organic Chemistry and Biotechnology: Past, Present, and Future, *J. Am. Chem. Soc.*, 2013, **135**, 12480–12496; (*c*) C. E. Humphrey, M. Ahmed, A. Ghanem and N. J. Turnerx, Application of Enzymes in Kinetic Resolutions, Dynamic Kinetic Resolutions and Deracemization Reactions, in *Separation of Enantiomers: Synthetic Methods*, ed. M. H. Todd, Wiley-VCH, Weinheim, Germany, 2014, ch. 4, pp. 123–160; (*d*) S. Wu, R. Snajdrova, J. C. Moore, K. Baldenius and U. T. Bornscheuer, Biocatalysis: Enzymatic Synthesis for Industrial Applications, *Angew. Chem., Int. Ed.*, 2021, **60**, 88–119; (*e*) Q. H. Zhang, Y. Fang, W. F. Luo and L. N. Huang, Biocatalytic Kinetic Resolution of D,L-pantolactone by Using a Novel Recombinant D-Lactonase, *RSC Adv.*, 2021, **11**, 721–725; (*f*) Q. H. Zhang, L. Yang, Y. B. Tang, L. N. Huang and W. F. Luo, Industrial Kinetic Resolution of D,L-Pantolactone by an Immobilized Whole-Cell Biocatalyst, *RSC Adv.*, 2021, **11**, 30373–30376.

6 (*a*) D. E. J. E. Robinson and S. D. Bull, Kinetic Resolution Strategies Using Non-Enzymatic Catalysts, *Tetrahedron: Asymmetry*, 2003, **14**, 1407–1446; (*b*) E. Vedejs and M. Jure, Efficiency in Nonenzymatic Kinetic Resolution, *Angew. Chem., Int. Ed.*, 2005, **44**, 3974–4001; (*c*) H. Pellissier, Catalytic Non-Enzymatic Kinetic Resolution, *Adv. Synth. Catal.*, 2011, **353**, 1613–1666.

7 (*a*) A. H. Hoveyda and M. T. Didiuk, Metal-Catalyzed Kinetic Resolution Processes, *Curr. Org. Chem.*, 1998, **2**, 489–526; (*b*) G. R. Cook, Transition Metal-Mediated Kinetic Resolution, *Curr. Org. Chem.*, 2000, **4**, 869–885; (*c*) L. Deng, Y. Fu, S. Y. Lee, C. Wang, P. Liu and G. Dong, Kinetic Resolution via Rh-Catalyzed C–C Activation of Cyclobutanones at Room Temperature, *J. Am. Chem. Soc.*, 2019, **141**, 16260–16265; (*d*) J. M. González, B. Cendón, J. L. Mascareñas and M. Gulías, Kinetic Resolution of Allyltriflamides through a Pd-Catalyzed C–H Functionalization with Allenes: Asymmetric Assembly of Tetrahydropyridines, *J. Am. Chem. Soc.*, 2021, **143**, 3747–3752.

8 (*a*) R. Gurubrahamam, Y.-S. Cheng, W.-Y. Huang and K. Chen, Recent Advances in Organocatalytic Kinetic Resolution for the Synthesis of Functionalized Products, *ChemCatChem*, 2016, **8**, 86–96 and references therein cited; (*b*) U. Farid, M. L. Aiello and S. J. Connon, Highly Enantioselective Catalytic Kinetic Resolution of α-Branched Aldehydes through Formal Cycloaddition with Homophthalic Anhydrides, *Chem. – Eur. J.*, 2019, **25**, 10074–10079; (*c*) S. Qu, S. M. Smith, V. Laina-Martín, R. M. Neyyappadath, M. D. Greenhalgh and A. D. Smith, Isothiourea-Catalyzed Acylative Kinetic Resolution of Tertiary α-Hydroxy Esters, *Angew. Chem., Int. Ed.*, 2020, **59**, 16572–16578; (*d*) J. Liu, L. Vasamsetty, M. Anwar, S. Yang, W. Xu, J. Liu, S. Nagaraju and X. Fang, Organocatalyzed Kinetic Resolution of α-Functionalized Ketones: The Malonate Unit Leads the Way, *ACS Catal.*, 2020, **10**, 2882–2893; (*e*) S. Sun, Z. Wang, S. Li, C. Zhou, L. Song, H. Huang and J. Sun, An Organocatalytic Kinetic Resolution of Aziridines by Thiol Nucleophiles, *Org. Lett.*, 2021, **23**, 554–558; (*f*) Y. Wu, M. Li, J. Sun, G. Zheng and Q. Zhang, Synthesis of Axially Chiral Aldehydes by N-Heterocyclic-Carbene-Catalyzed Desymmetrization Followed by Kinetic Resolution, *Angew. Chem., Int. Ed.*, 2022, **61**, e202117340; (*g*) S. Barik, R. C. Das, K. Balanna and A. T. Biju, Kinetic Resolution Approach to the Synthesis of C–N Axially Chiral N-Aryl Aminomaleimides via NHC-Catalyzed [3+3] Annulation, *Org. Lett.*, 2022, **24**, 5456–5461.

9 A. Suárez, C. W. Downey and G. C. Fu, Kinetic Resolutions of Azomethine Imines via Copper-Catalyzed [3+2] Cycloadditions, *J. Am. Chem. Soc.*, 2005, **127**, 11244–11245.

10 (*a*) H. Takayama, Z.-J. Jia, L. Kremer, J. O. Bauer, C. Strohmann, S. Ziegler, A. P. Antonchick and

H. Waldmann, Discovery of Inhibitors of the Wnt and Hedgehog Signaling Pathways through the Catalytic Enantioselective Synthesis of an Iridoid-Inspired Compound Collection, *Angew. Chem., Int. Ed.*, 2013, **52**, 12404–12408; (*b*) H. Xu, C. Golz, C. Strohmann, A. P. Antonchick and H. Waldmann, Enantiodivergent Combination of Natural Product Scaffolds Enabled by Catalytic Enantioselective Cycloaddition, *Angew. Chem., Int. Ed.*, 2016, **55**, 7761–7765; (*c*) Y. Yuan, Z.-J. Zheng, L. Li, X.-F. Bai, Z. Xu, Y.-M. Cui, J. Cao, K.-F. Yang and L.-W. Xu, Silicon-based Bulky Group–Tuned Parallel Kinetic Resolution in Copper-Catalyzed 1,3-Dipolar Additions, *Adv. Synth. Catal.*, 2018, **360**, 3002–3008; (*d*) C. Shen, Y. Yang, L. Wei, W.-W. Dong, L. W. Chung and C.-J. Wang, Kinetic Resolution of Alkylidene Norcamphors via a Ligand-Controlled Umpolung-Type 1,3-Dipolar Cycloaddition, *iScience*, 2019, **11**, 146–159; (*e*) H. Deng, T.-T. Liu, Z.-D. Ding, W.-L. Yang, X. Luo and W.-P. Deng, Kinetic resolution of 2H-azirines via Cu(I)-catalyzed asymmetric 1,3-dipolar cycloaddition of azomethine ylides, *Org. Chem. Front.*, 2020, **7**, 3247–3252.

11 J.-W. Xie, L.-P. Fan, H. Su, X.-S. Li and D.-C. Xu, Efficient kinetic resolution of racemic 3-nitro-2H-chromene derivatives catalyzed by Takemoto's organocatalyst, *Org. Biomol. Chem.*, 2010, **8**, 2117–2122.

12 J. Yu, W.-J. Chen and L.-Z. Gong, Kinetic Resolution of Racemic 2,3-Allenoates by Organocatalytic Asymmetric 1,3-Dipolar Cycloaddition, *Org. Lett.*, 2010, **12**, 4050–4053.

13 A. Husain, S. A. Khan, F. Iram, M. A. Iqbal and M. Asif, Insights into the chemistry and therapeutic potential of furanones: A versatile pharmacophore, *Eur. J. Med. Chem.*, 2019, **171**, 66–92 and references cited therein.

14 (*a*) F. Fariña, M. V. Martín and F. Sánchez, Pseudoesters and Derivatives. XXIV. 1,3-Dipolar Cycloaddition of Diazomethane to 5-Methoxyfuran-2(5*H*)-ones, *Heterocycles*, 1986, **24**, 2587–2592; (*b*) L. Fišera and P. Oravec, Stereoselectivity of Cycloadditions of Arylnitrile Oxides to 5-Alkoxy-2(5*H*)-furanone, *Collect. Czech. Chem. Commun.*, 1987, **52**, 1315–1324; (*c*) B. L. Feringa and B. de Lange, Asymmetric 1,4-Additions to 5-Alkoxy-2(5*H*)-furanones: An Efficient Synthesis of (*R*)- and (*S*,)-3,4-Epoxy-1-Butanol, *Tetrahedron*, 1988, **44**, 7213–7222; (*d*) B. L. Feringa and B. de Lange, 1,4-Additions of Amines to 5-Methoxyfuran-2(5*H*)-one; an Efficient Synthesis of Amino Diols, *Heterocycles*, 1988, **27**, 1197–1205; (*e*) E. Keller, B. de Lange, M. T. Rispens and B. L. Feringa, 1,3-Dipolar Cycloadditions to 5-Methoxy-2(5*H*)-furanone, *Tetrahedron*, 1993, **49**, 8899–8910; (*f*) F. Fariña, M. R. Martín, M. V. Martín and A. Martinez de Guereñu, Cycloaddition of Nitrile Oxides to 4-Oxobut-2-enoic Acid Derivatives, *Heterocycles*, 1994, **38**, 1307–1316; (*g*) W. S. Faber, J. Kok, B. de Lange and B. L. Feringa, Catalytic Kinetic Resolution of 5-Alkoxy-2(5*H*)-furanones, *Tetrahedron*, 1994, **50**, 4775–4794.

15 (*a*) J. L. García Ruano, A. Fraile, M. R. Martín and A. Núñez, First Asymmetric Cycloaddition of Carbonyl Ylides to Vinyl Sulfoxides and Furan-2(5*H*)-ones, *J. Org. Chem.*, 2006, **71**, 6536–6541; (*b*) A. Núñez Jr., M. R. Martín, A. Fraile and J. L. García Ruano, Abnormal Behaviour of Allenylsulfones under Lu's Reaction Conditions: Synthesis of Enantiopure Polyfunctionalised Cyclopentenes, *Chem. – Eur. J.*, 2010, **16**, 5443–5453; (*c*) J. L. García Ruano, A. Fraile, M. R. Martín, G. González, C. Fajardo and A. M. Martín-Castro, Asymmetric Synthesis of Pyrrolo[2,1-*a*]isoquinoline Derivatives by 1,3-Dipolar Cycloadditions of Stabilized Isoquinolinium *N*-Ylides with Sulfinyl Dipolarophiles, *J. Org. Chem.*, 2011, **76**, 3296–3305.

16 (*a*) B. L. Feringa and J. C. de Jong, New Strategies in Asymmetric Synthesis Based on γ-Alkoxybutenolides, *Bull. Soc. Chim. Belg.*, 1992, **101**, 627–640; (*b*) B. L. Feringa, B. de Lange, J. F. G. A. Jansen, J. C. de Jong, M. Lubben, W. Faber and E. P. Schudde, New Approaches in Asymmetric Synthesis Using γ-Alkoxybutenolides, *Pure Appl. Chem.*, 1992, **64**, 1865–1871 and references cited therein.

17 (*a*) D. M. Cooper, R. Grigg, S. Hargreaves, P. Kennewell and J. Redpath, X=Y-ZH Compounds as Potential 1,3-Dipoles. Part 44.[1] Asymmetric 1,3-Dipolar Cycloaddition Reactions of Imines and Chiral Cyclic Dipolarophiles, *Tetrahedron*, 1995, **51**, 7791–7808; (*b*) H. A. Dondas, R. Grigg and M. Thornton-Pett, Spiro(Pyrrolidinyl-2,3′-Benzodiazepines) Related to MK-329, *Tetrahedron*, 1996, **52**, 13455–13466; (*c*) B. M. Trost and M. L. Crawley, A "Chiral Aldehyde" Equivalent as a Building Block Towards Biologically Active Targets, *Chem. – Eur. J.*, 2004, **10**, 2237–2252; (*d*) R. Grigg, D. M. Cooper, S. Holloway, S. McDonald, E. Millingtona and M. A. B. Sarker, X=Y–ZH Systems as Potential 1,3-Dipoles. Part 61: Metal Exchanged Zeolites, Silver(I) Oxide, Ni(II) and Cu(I) Complexes as Catalysts for 1,3-Dipolar Cycloaddition Reactions of Imines Generating Proline Derivatives, *Tetrahedron*, 2005, **61**, 8677–8685.

18 (*a*) J. L. García Ruano, A. Fraile and M. R. Martín, (*Ss*)-5-Ethoxy-3-*p*-Tolylsulfinylfuran-2(5*H*)-ones as Chiral Dipolarophiles: First Asymmetric Cycloaddition of Diazomethane to Vinyl Sulfoxides, *Tetrahedron: Asymmetry*, 1996, **7**, 1943–1950; (*b*) J. L. García Ruano, J. I. Andrés Gil, A. Fraile, A. M. Martín Castro and M. R. Martín, Asymmetric 1,3-Dipolar Reactions of 3-Sulfinylfuran-2(5*H*)-ones with 11*H*-Dibenzo[*b*,*e*]azepine 5-Oxide. Synthesis of Pyrroloazepines via Isoxazoloazepines, *Tetrahedron Lett.*, 2004, **45**, 4653–4656; (*c*) J. L. García Ruano, A. Fraile, A. M. Martín Castro and M. R. Martín, The Role of the Sulfinyl Group on the Course of the Reactions of 3-*p*-Tolylsulfinylfuran-2(5*H*)-ones with Nitrones. Synthetic Uses of Cycloreversion Processes, *J. Org. Chem.*, 2005, **70**, 8825–8834; (*d*) J. L. García Ruano, A. Núñez Jr., M. R. Martín and A. Fraile, Totally Regio- and Stereoselective Behavior of Mono- and Diactivated Cyclic Alkenes in the Lu Reaction: Synthesis of Enantiopure Functionalized Cyclopentanes, *J. Org. Chem.*, 2008, **73**, 9366–9371.

19 *Green Chemistry: Theory and Practice*, ed. P. T. Anastas and J. C. Warner, Oxford University Press, 1998.

20 D. G. Blackmond, Kinetic Resolution Using Enantioimpure Catalysts: Mechanistic Considerations of Complex Rate Laws, *J. Am. Chem. Soc.*, 2001, **123**, 545–553.

21 (*a*) A. Guerrero-Corella, M. A. Valle-Amores, A. Fraile and J. Alemán, Enantioselective Organocatalyzed aza-Michael Addition Reaction of 2-Hydroxybenzophenone Imines to Nitroolefins under Batch and Flow Conditions, *Adv. Synth. Catal.*, 2021, **363**, 3845–3851; (*b*) F. Esteban, W. Cieslik, E. M. Arpa, A. Guerrero-Corella, S. Díaz-Tendero, J. Perles, J. A. Fernández-Salas, A. Fraile and J. Alemán, Intramolecular Hydrogen Bond Activation: Thiourea-Organocatalyzed Enantioselective 1,3-Dipolar Cycloaddition of Salicylaldehyde-Derived Azomethine Ylides with Nitroalkenes, *ACS Catal.*, 2018, **8**, 1884–1890; (*c*) A. Guerrero-Corella, A. Fraile and J. Alemán, Intramolecular Hydrogen-Bond Activation: Strategies, Benefits, and Influence in Catalysis, *ACS Org. Inorg. Au*, 2022, **2**, 197–204.

22 A. Guerrero-Corella, F. Esteban, M. Iniesta, A. Martín-Somer, M. Parra, S. Díaz-Tendero, A. Fraile and J. Alemán, 2-Hydroxybenzophenone as a Chemical Auxiliary for the Activation of Ketiminoesters for Highly Enantioselective Addition to Nitroalkenes under Bifunctional Catalysis, *Angew. Chem., Int. Ed.*, 2018, **57**, 5350–5354.

23 CCDC 2160961‡ (**4i**) contains the supplementary crystallographic data for this paper.

24 F. Fariña and M. D. Parellada, Pseudoesters and Derivatives. 29. Regioselective Reactions of the 5-(Ethylthio) furan-2(5H)-one Anion with Electrophiles, *J. Org. Chem.*, 1988, **53**, 3330–3333.

25 (*a*) All the optimized structures computed can be visualized and downloaded from **https://dx.doi.org/10.19061/iochem-bd-8-10**; (*b*) M. Álvarez-Moreno, C. de Graaf, N. Lopez, F. Maseras, J. M. Poblet and C. Bo, Managing the Computational Chemistry Big Data Problem: The ioChem-BD Platform, *J. Chem. Inf. Model.*, 2015, **55**, 95–103.

26 I. Iribarren and C. Trujillo, Efficiency and Suitability when Exploring the Conformational Space of Phase-Transfer Catalysts, *J. Chem. Inf. Model.*, 2022, **62**, 5568–5580.

27 C. Bannwarth, S. Ehlert and S. Grimme, GFN2-xTB–An Accurate and Broadly Parametrized Self-Consistent Tight-Binding Quantum Chemical Method with Multipole Electrostatics and Density-Dependent Dispersion Contributions, *J. Chem. Theory Comput.*, 2019, **15**, 1652–1671.

28 P. Pracht, F. Bohle and S. Grimme, Automated Exploration of the Low-Energy Chemical Space with Fast Quantum Chemical Methods, *Phys. Chem. Chem. Phys.*, 2020, **22**, 7169–7192.

29 S. Grimme, S. Ehrlich and L. Goerigk, Effect of the Damping Function in Dispersion Corrected Density Functional Theory, *J. Comput. Chem.*, 2011, **32**, 1456–1465.

30 M. J. Frisch, *et al.*, *Gaussian 16, Revision C.01*, Gaussian, Inc., Wallingford, CT, 2019.

31 (*a*) E. R. Johnson, S. Keinan, P. Mori-Sanchez, J. Contreras-García, A. J. Cohen and W. Yang, Revealing Noncovalent Interactions, *J. Am. Chem. Soc.*, 2010, **132**, 6498–6506; (*b*) J. Contreras-García, E. R. Johnson, S. Keinan, R. Chaudret, J.-P. Piquemal, D. N. Beratan and W. Yang, NCIPLOT: A Program for Plotting Non-Covalent Interaction Regions, *J. Chem. Theory Comput.*, 2011, **7**, 625–632.